GSK3β Inhibition Synergizes with PARP Inhibitors through the Induction of Homologous Recombination Deficiency in Colorectal Cancer

Ning Zhang
Shanghai Institute of Materia Medica Chinese Academy of Sciences
Yu-Nan Tian
Shanghai Institute of Materia Medica Chinese Academy of Sciences
Li-Na Zhou
Shanghai Institute of Materia Medica Chinese Academy of Sciences
Meng-Zhu Li
Shanghai Institute of Materia Medica Chinese Academy of Sciences
Shan-Shan Song
Shanghai Institute of Materia Medica Chinese Academy of Sciences
Xia-Juan Huan
Shanghai Institute of Materia Medica Chinese Academy of Sciences
Xu-Bing Bao
Shanghai Institute of Materia Medica Chinese Academy of Sciences
Ao Zhang
Shanghai Institute of Materia Medica Chinese Academy of Sciences
Ze-Hong Miao
Shanghai Institute of Materia Medica Chinese Academy of Sciences
Jin-Xue He (jinxue_he@simm.ac.cn)
Shanghai Institute of Materia Medica Chinese Academy of Sciences

Research

Keywords: PARP inhibitor, GSK3β, homologous recombination repair, BRCA1, colorectal cancer

Posted Date: August 1st, 2020

DOI: https://doi.org/10.21203/rs.3.rs-48785/v1

Abstract

Background: Monotherapy with poly ADP-ribose polymerase (PARP) inhibitors results in limited objective response rate (≤ 60% in most cases) in patients with homologous recombination repair (HRR)-deficient cancer, which suggests a high rate of resistance in this subset of patients to PARP inhibitors (PARPi). To overcome resistance to PARPi and to broaden their clinical use, we performed high-throughput screening of 99 anticancer drugs in combination with PARPi to identify potential therapeutic combinations.

Methods: The effects of PARPi combined with glycogen synthase kinase 3 (GSK3) inhibitors were investigated *in vitro* with respect to cell viability, cell cycle and apoptosis. The synergy was assessed by calculation of the combination index (CI). *GSK3α* null and *GSK3β* null cells were generated using CRISPR/Cas9 technique. The underlying mechanism was examined by western blotting, flow cytometry, qRT-PCR and fluorescence microscopy. This combination was also evaluated in the mouse xenograft model; tumor growth and tumor lysates were analyzed, and the immunohistochemistry assay was performed. All data are presented as mean ± SD. Comparison between two groups was performed with the Student's *t*-test.

Result: The data showed that ~25% of oncological drugs and kinase inhibitors that were evaluated displayed synergy with PARPi in HCT-15 cells. Among the tested agents, GSK3 inhibitors (GSK3i) exhibited the strongest synergistic effect with PARPi. Moreover, the synergistic antitumor effect of GSK3 and PARP inhibition was confirmed in a panel of colorectal cancer (CRC) cell lines with diverse genetic backgrounds. Additionally, inhibition or genetic depletion of GSK3β was found to impair HRR of DNA and reduce the mRNA and protein level of BRCA1. Finally, we demonstrated that inhibition or depletion of GSK3β could enhance the *in vivo* sensitivity to simmiparib without toxicity.

Conclusion: Our results provide a mechanistic understanding of combination of PARP and GSK3 inhibition, and support the clinical development of this combination therapy for CRC patients.

Background

Poly (ADP-ribose) polymerases (PARP) are important DNA repair enzymes [1]. PARP inhibitors (PARPi) including olaparib, niraparib, rucaparib and talazoparib have been approved as monotherapy for patients with *BRCA1/2*-mutated ovarian cancers, breast cancer, pancreatic cancer and prostate cancer [2, 3]. Despite promising clinical results, as with other targeted drugs, the efficacy of PARPi is limited by the drug resistance. Only a fraction of *BRCA1/2* mutation carriers responded to PARPi, and even those who responded subsequently developed resistance and relapsed [4, 5]. Furthermore, the promise of PARPi in the management of BRCA1/2-deficient cancers is tempered by the fact that homologous recombination (HR)-proficient tumors do not respond to these agents. Thus, the development of strategies to selectively impair HR in cancer cells and subsequently sensitize the PARPi resistance of BRCA-deficient cancers and HR-proficient cancers to PARP inhibition may provide new clinical applications. In this regard, drug combination approaches have been designed and evaluated in preclinical and early clinical trials [6].

Currently, the combination of olaparib and bevacizumab has been approved for patients with advanced ovarian cancer [7].

PARPi are thought to trap the PARP1/2 enzymes at site of DNA damage, leading to replication-induced DNA damage that requires BRCA1/2-dependent homologous recombination repair (HRR) [8]. Therefore, DNA-damaging agents and molecular inhibitors that target DNA damage response pathways, such as ATR and Chk1, are expected to enhance the antitumor effect of PARPi [9, 10]. PARPi in combination with other targeted therapies that are capable of disrupting HRR have also shown promising results in preclinical studies [6]. However, clinical studies showed that PARPi in combination with cytotoxic chemotherapies (such as topotecan, cisplatin, gemcitabine and temozolomide) had limited clinical efficacy and high toxicity [11–14]. Therefore, new combination strategies are needed to improve the efficacy and alleviate the toxicity of combination therapy.

Clinical studies showed that more than 40% of BRCA1/2-deficient patients failed to respond to PARPi, which meant a high rate of *de novo* resistance to PARP inhibition even among in *BRCA*-mutated tumors [4, 5]. Previous data revealed that PARPi including olaparib, niraparib and simmiparib induced mild synthetic lethality in human breast cancer, HCC1937 (BRCA1-deficient), and colorectal cancers (CRC), HCT-15 (BRCA2-deficient), cells *in vitro*, and the antitumor activity was limited in mouse xenograft models [15–17]. Thus, HCC1937 and HCT-15 cells serve as model cell lines for *de novo* resistance to PARP inhibition. Specially, majority of studies focused on a specific drug and PARP inhibition-induced alterations of its efficacy in BRCA-proficient cancer cells. As such, relatively little is known about the BRCA1/2 deficiency on PARPi-based combination and how PARPi alters the efficacy of a broad spectrum of drugs.

In this study, new combinatorial therapy strategies were investigated to improve the anticancer efficacy in *BRCA*-mutated cells with primary PARPi resistance. We first performed a preliminary screening of 99 anticancer drugs in combination with the PARPi, olaparib and niraparib, in HCC1937 or HCT-15 cells. The results revealed that inhibition of PARP partly affected the cellular sensitivity to a panel of oncological drugs and kinase inhibitors. Among these agents, glycogen synthase kinase 3 (GSK3) inhibitors (GSK3i) exhibited the best synergistic effect with PARPi in BRCA2-deficient HCT-15 cells. Moreover, the data showed that the PARPi, simmiparib, acted synergistically with the GSK3i, CHIR99021 HCl and LY2090314, in a panel of BRCA-proficient CRC cells. These results indicated that combination of GSK3i and PARPi may serve as a new therapeutic strategy for CRC patients.

Materials And Methods

Antibodies and chemicals

Simmiparib was provided by Dr. Ao Zhang and prepared as described previously [18]. Olaparib, talazoparib, niraparib, rucaparib, irinotecan, adriamycin, etoposide, and the ninety-nine inhibitors (listed in Table S1) used for combination screening were purchased from Selleck Chemicals (Houston, TX, USA). Antibodies against Mre11 (sc-5858), CtIP (sc-271339), BRCA1 (sc-642), Rad52 (sc-8530), and Rad51 (sc-

8349) were from Santa Cruz Biotechnology (Santa Cruz, CA, USA). Antibodies against γH2AX (80312), GSK3α (4337), GSK3β (12456), cleaved-Caspase3 (9661), cleaved-PARP1 (5625), and RPA32 (2208) were from Cell Signaling Technology (Danvers, MA, USA). Anti-GAPDH (AG019) antibody was from Beyotime (Shanghai, China).

Cell lines

Human HCC1937, HCT-15, RKO, HCT-116, and HT-29 cell lines were purchased from the American Type Culture Collection (Manassas, VA, USA). SW480 and SW620 cell lines were obtained from the Cell Bank of the Chinese Academy of Sciences Type Culture Collection (Shanghai, China). DR-U2OS cells were gifted by Ming Huang (Shanghai Institute of Materia Medica). Cells were cultured according to the supplier's instructions and authenticated by short tandem repeat (STR) analysis performed by Genesky.

Screening of drug combinations

BRCA1-deficient HCC1937 and BRCA2-deficient HCT-15 cells were used for screening the drug combinations. Prior to screening, olaparib and niraparib were arrayed in 96-well plates and serially diluted 2-fold to obtain a concentration that was 20% of inhibition rate (IR) of olaparib and niraparib. Sulforhodamine B (SRB) assay was used to analyze cytotoxicity. For combination screening, cells were plated and then treated with the various agents at three concentrations, covering a 100-fold concentration range, with or without a fixed concentration of olaparib or niraparib (~20% IR). The IRs of the various agents, PARPi and combinations were defined as IR1, IR2, and IR3, respectively. The combination effect was calculated using the IR values and equalled to IR3-IR2-IR1, which was defined by the color intensity (green [0% inhibition] to red [100% inhibition]).

Generation of *GSK3α* and *GSK3β* KO cells using CRISPR/Cas9

Lentiviral transfection of cultured cells with pLentiCRISPRv2 vectors encoding *GSK3α* and *GSK3β*-specific CRISPR or control vectors (Obio Technology Co., Ltd., Shanghai, China) was performed according to the supplier's instructions. The sequences of the oligonucleotide sgRNAs designed for *GSK3α* and *GSK3β* were 5'-ACCGggcgcggactagctcgttcg-3' and 5'-ACCGgcccagaaccacctcctttg-3'. The oligos were annealed and inserted into the lentiviral vector pLenti-U6-spgRNA v2.0-CMV-Puro-P2A-3Flag-spCas9. 293T cells were transfected with 7.5 μg psPAX2, 2.5 μg pMD2.G and 10 μg pLentiCRISPRv2 *GSK3α/β* sgRNA or pLentiCRISPRv2 vector. HCT-15 and RKO cells were then transduced with the lentiviruses. Finally, complete ablation of GSK3α or GSK3β expression was verified in the single cell clones using western blotting.

Cytotoxicity assays and combination analysis

Cells were treated with the indicated drug combinations and the IR on cell proliferation was determined using SRB assays as described previously [19].

Combination Index (CI) was analyzed using the CalcuSyn software with the Chou-Talalay equation [20]. CI < 1, CI = 1, and CI > 1 represented synergism, additive effect and antagonism, respectively.

Flow cytometry

Cells were prepared for the analysis of cell cycle distribution or apoptosis as described previously [21]. Data were collected using a FACS Calibur Instrument (BD Biosciences, Franklin Lake, NJ, USA) and analyzed with the FlowJo software.

Colony formation assay

Cells were plated in 6-well plates, cultured for 12 h, and then treated with various concentration of drugs for another 7 d. After fixing, the colonies were stained with SRB and the optical density value was measured at 560 nm using a microplate reader (Molecular Devices, Sunnyvale, CA, USA).

RNA interference

All small siRNAs were purchased from Genepharma (Shanghai, China). Transfection was conducted using Lipofectamine RNAiMAX (Invitrogen; Carlsbad, CA, USA) following the manufacture's guidance. The sequences were as follows: negative control siRNA (si*NC*), 5'-UUCUCCGAACGUGUCACGUTT-3'; si*GSK3β*#1, 5'-GCUAGAUCACUGUAACAUATT-3'; si*GSK3β*#2, 5'-GAAAGCT AGATCACTTT-3'; si*GSK3α*#1, 5'-CCAGGACAAGAGGTTCAAGAA-3'; si*GSK 3α*#2, 5'-CCCCTGGACAAAGGTGTTCAAAT-3'.

Transfection with GSK3β plasmids

Wild type (WT) or mutant GSK3β reconstituted cells were generated using lentiviral transfection of *GSK3β* KO1 HCT-15 cells with pLenti vectors encoding *GSK3β* WT or *GSK3β* Y216F cDNA (Obio Technology Co. Ltd.) followed by selection in presence of blasticidin.

The Flag-GSK3β WT plasmid was purchased from Obio Technology Co. Ltd. HCT-15 cells were transfected with the plasmid using lipofectamine 3000 (Invitrogen; Carlsbad, CA, USA) according to the manufacturer's instructions.

Immunofluorescence

Cells were prepared for immunofluorescence analysis as described previously [22]. Finally, the cells were stained with DAPI and imaged with a Leica immunofluorescence microscope (TCS-SP8 STED, Leica, Germany). The percentage of γH2AX and RAD51 foci positive cells (≥ 5 foci/cell) was calculated based on the analysis of randomly chosen fields which included at least 50 cells.

HR repair assay

HR repair assays were performed as described previously using the DR-U2OS reporter cell line [23]. Quantification was performed using 10,000 cells collected per sample. To examine the role of GSK3i or

individual genes in DNA double-strand breaks (DSBs) repair, the cells were treated with the indicated agents or transfected with siRNA for 24 h. Then, the cells were transfected with a plasmid expressing I-SceI (pCBASce) for 48 h. GFP-positive cells were quantified using flow cytometry.

Western blotting

Standard western blotting protocol was used to measure the cellular level of the indicated proteins, as described previously [17].

Quantitative real-time PCR

Total RNA was extracted using HiPure Total RNA Mini Kit (Magen, Guangzhou, China) according to the manufacturer's protocol. cDNA was generated using a RT reagent kit (TaKaRa, Tokyo, Japan). The quantitative real-time reverse transcription polymerase chain reaction (qRT-PCR) reactions were performed using a 7500 Fast Real-time PCR System (Applied Biosystem, Grand Island, NY, USA). The primer sequences were as follows: 5'-ACCTTGGAACTGTGAGAACTCT-3' (forward) and 5'-TCTTGATCTCCCACACTGCAATA-3' (reverse) for *BRCA1*; 5'-GAGAAGGCTGGGGCTCATTT-3' (forward) and 5'-AGTGATGGCATGGACTGTGG -3' (reverse) for *GAPDH*. All experiments were performed in triplicate and normalized to the *GAPDH* transcript levels using the comparative CT method.

In vivo anticancer activity experiments

Female nu/nu athymic BALB/cA mice (aged 5-6 weeks) were obtained from GemPharmatech (Jiangsu, China). All studies were conducted in compliance with the Institutional Animal Care and Use Committee guidelines of the Shanghai Institute of Materia Medica (Shanghai, China).

HCT-15, RKO, and HCT-15 KO xenografts were established by inoculating 5×10^6 cells subcutaneously in the nude mice. When the xenografts reached a volume of 60–100 mm^3, the mice were randomized into control and treatment groups as indicated. Simmiparib and LY2090314 alone or in a combination were injected every other day for the indicated period. Tumor growth was monitored by the measuring the tumor size using calipers every other day and the tumor volume was calculated using the formula (length × $width^2$)/2. Tumor tissues were collected 2 h after final dosing for immunoblotting or immunohistochemical staining. Images of immunohistochemical staining were captured using a NanoZoomer S210 (Hamamatsu, Japan) and processed using the NDP.scan.3.2.15 software.

Statistical analyzes

All data are presented as mean ± standard deviation (SD). Comparison between two groups was performed using the Student's *t*-test. $p < 0.05$ was considered to be statistically significant.

Results

Drug combination screen identifies GSK3i as acting synergistically with PARPi

To explore whether small-molecule inhibitors can sensitize cancer cells to PARPi, we performed a drug combination screen in BRCA1-deficient breast cancer cell line of HCC1937 and BRCA2-deficient CRC cell line of HCT-15, which express mutant-type BRCA1 or BRCA2 protein but modestly respond to PARPi. FDA-approved PARPi (Olaparib and Niraparib) and 99 well-characterized anticancer drugs targeting fifty classes of proteins belonging to indicated different kind of signaling pathway were chosen for initial screen (Table S1). Strikingly, a strong synergistic effect of GSK3i (CHIR99021 HCl and LY2090314) and PARPi (Olaparib and Niraparib) was observed in HCT-15 cells (Figure 1A). Unsurprisingly, ATR inhibitors and CHEK1 inhibitors showed synergistic effects with PARPi (Olaparib and Niraparib) in HCC1937 and HCT-15 cells, which had been reported that both ATR and CHEK1 inhibitors increased the sensitivity to PARPi in a BRCA1-independent way [9, 10]. Moreover, prior studies have demonstrated that inhibitor of BET, CDK1, HDAC, Protease, PI3K, and VEGFR could all decrease BRCA1 and other HRR factors at the protein level, thereby increasing the sensitivity of the cancer cell lines to PARP inhibition [24-29]. Consistent with the above conclusion, we found that these inhibitors displayed a synergistic effect with Olaparib and Niraparib in HCT-15 cells (Figure 1A). As reported [30-33], we also observed that Olaparib and Niraparib showed a synergistic effect in combination with inhibitors of DNMT, DNA-PK, mTOR, and HDM in HCT-15 cells (Figure 1A).

To further confirm the accuracy of our screening results, we validated the above results in the combination of Olaparib and CDK1 inhibitor (RO-3306) or ATR inhibitor (VE821) using the CalcuSyn model. Both combinations (*i.e.*, olaparib + RO-3306 and olaparib + VE-821) caused obvious synergistic effects (CI < 0.7) in BRCA2-deficient HCT-15 cells, while only the olaparib and VE-821 combination produced synergistic effect (CI < 0.6) in the BRCA1-deficient HCC1937 cells (Figure 1B and 1C). These data were consistent with the observation shown in Figure 1A.

GSK3 inhibition sensitizes BRCA-proficient CRC cells to PARPi

We next sought to validate the observed interactions between GSK3 activity and PARPi. To further investigate the effect of GSK3 activity on cellular response to PARPi, two specific GSK3i, LY2090314 (LY) and CHIR99021 HCl (CHIR), were used in combination with five PARPi, including olaparib, niraparib, rucaparib, talazoparib and simmiparib. To exclude the synergistic effects were simply due to cell cycle arrest, we chose the concentrations of GSK3i (CHIR $\leq$ 10 μM; LY $\leq$ 5 μM) that had no discernible effect on cell proliferation (Figure S1A) and cell cycle phasing. Cells were treated with PARPi at eight concentrations, with or without LY2090314 or CHIR99021 HCl. The data showed that GSK3 inhibition strongly synergized with simmiparib (SP), talazoparib (TP), olaparib (OP), rucaparib (RP) and niraparib (NP) in HCT-15 cells (Figure 2A). The synergistic effect decreased in the order of simmiparib (sensitive fold: up to ~4463-fold), talazoparib (~185-fold), olaparib (~10-fold), niraparib (~4-fold) and rucaparib (~3-fold) when combined with LY2090314. Thus, simmiparib, a potent and selective PARP inhibitor currently in phase I clinical trials in China, was the most strongly perturbed following GSK3 inhibition (No. CTR20160475). Moreover, the presence of GSK3i led to a decrease IC_{50} of simmiparib in a concentration-dependent manner in HCT-15 cells (Figure 2B and Figure S1B). In line with the synergistic effects between simmiparib and GSK3i, we observed enhanced G2/M arrest and apoptotic cell death induced by

simmiparib when combined with LY2090314 (Figure 2C-E) or CHIR99021 HCl (Figure S1C-E). The protein levels of cleaved PARP1 (p85) and cleaved-Caspase 3 increased accordingly (Figure 2F and Figure S1F). The results indicated that simmiparib and GSK3i combination treatment significantly suppressed tumor cell growth, caused cells to accumulate in G2/M of the cell cycle and induced remarkably apoptotic response.

To determine whether these synergies extend across other tumor cells, we used additional BRCA-proficient CRC cell lines (RKO, HCT-116, SW480, SW620, and HT-29). The data showed that GSK3 inhibition strongly synergized with simmiparib in all the BRCA-proficient CRC cells (CI < 0.6), as well as HCT-15 cells (Figure 2G and Figure S1G). Consistently, no combination activity (CI > 1) was observed in BRCA1-deficient HCC1937 cell lines (Figure S1H). This finding suggested a broader benefit of PARPi combined with GSK3i in BRCA-proficient CRC cells.

GSK3β depletion selectively sensitizes cancer cells to PARP and topoisomerase (Top) I inhibitors

There are two highly homologous forms of GSK3 in human, GSK3α and GSK3β, that have different tissue-specific functions and substrates [34, 35]. As GSK3i (LY2090314 and CHIR99021 HCl) block both GSK3α and GSK3β activity, we next generated *GSK3α* null and *GSK3β* null cells lines using CRISPR/Cas9 technique in HCT-15 and RKO cells, respectively (Figure 3A and 3B). Relative to the parental cells, the *GSK3β* KO cells (#KO1 and #KO2) displayed up to 60-fold increased sensitivity to the PARPi, simmiparib (Figure 3C and 3D). However, GSK3α depletion did not affect the cellular sensitivity to PARPi (Figure 3E). These results indicated that depletion of GSK3β selectively sensitized cancer cells to PARPi.

To investigate the possible involvement of GSK3β in sustaining genomic stability, we examined whether GSK3i, LY2090314, synergized with different DNA-damaging agents known to generate different forms of DNA lesions in HCT-15 cell line. The results revealed that GSK3i synergized with irinotecan (CPT-11, Top I inhibitor; CI < 0.4), but not adriamycin (ADR, Top II inhibitor; CI > 1) or etoposide (VP-16, Top II inhibitor; CI > 1) (Figure S2A and S2B). Similarly, GSK3β depletion, but not GSK3α, significantly increased the cellular sensitivity to CPT-11 (Figure S2C and S2D).

GSK3β is required for the HRR of DSBs

Although PARPi and Top I inhibitor cause different forms of DNA lesions, both agents are known to selectively kill proliferating cancer cells by causing replication-dependent DSBs [36, 37]. For this reason, we compared the occurrence of drug-induced DSBs in *GSK3β* KO and parental cells, using γH2AX as a marker. Higher level of γH2AX protein accumulated in *GSK3β* KO cells compared to the parental cells (Figure 4A and Figure S3A). This result was further supported by the enhanced γH2AX protein level in cells treated with a combination PARPi and GSK3i (Figure 4B and Figure S3B); and the observation was recapitulated using an immunofluorescence assay to stain nuclear γH2AX foci (Figure 4C and Figure S3C). However, the level of DSBs was similarly induced in *GSK3α* null cells and parental cells (Figure S3D). These results indicated that a defect in DSBs repair was caused by the knockout of GSK3β, but not GSK3α.

Replication-dependent DSBs lesions are known to be predominantly repaired by HR, a repair process requiring homologous DNA sequence as a template. To test whether GSK3β inhibition and knockdown cells were defective in HRR, we chose a well-characterized reporter assay using the DR-U2OS, a human osteosarcoma cell line with chromosomally integrated HR reporter gene containing an I-SceI recognition sequence [23]. In this cell line, HRR using a direct repeat within the reporter cassette as a template results in an intact GFP gene, which can be detected by flow cytometry. The data showed that GSK3β knockdown using two independent siRNAs remarkably decreased the HR efficiency triggered by I-SceI (Figure 4D). Consistently, the GSK3i, CHIR99021 HCl and LY2090314, significantly reduced the capacity of HRR, in which ATR inhibitor, VE821, was used as a positive control (Figure 4E). However, GSK3α silencing had no impact on HR efficiency (Figure S3E). Additionally, we observed impaired RAD51 foci formation in *GSK3β* KO cells or GSK3i-treated cells which further strengthened the deficiency in HRR (Figure 4F and Figure S3F). Together, these data identified a previously unappreciated role of GSK3β in HRR, which echoed our findings that GSK3β inhibition and depletion affected cell sensitivity to PARP and Top I inhibitors.

GSK3β depletion represses the expression of BRCA1

To understand how GSK3β is involved in HRR, we analyzed the protein level of the key factors involved in the HR pathways using western blotting. *GSK3β* KO cells showed a marked reduction in BRCA1 protein levels, whereas the levels of Mre11, CtIP, RPA32 and RAD52 were not affected (Figure 5A and Figure S4A). Similarly, inactivation of GSK3β by CHIR99021 HCl and LY2090314 treatment led to a marked decrease in BRCA1 protein level in a concentration- and time-dependent manner (Figure 5B and 5C; Figure S4B and S4C). Furthermore, we found that GSK3β depletion and inhibition reduced RAD51 protein level in HCT-15 cells but not in RKO cells (Figure5A and 5B, Figure S4A and S4B). Therefore, we assessed the effect of LY2090314 on BRCA1 and RAD51 protein levels in other CRC cells (HCT116, HT29, SW480 and SW620). LY2090314 modestly decreased RAD51 level in HT-29 cells, while it consistently decreased BRCA1 protein in all the lines assessed (Figure S4D). We thus focused on BRCA1 as a likely mediator of the GSK3i effect. We transfected *WT-GSK3β* (WT) or a kinase-inactive mutant *GSK3β*^{Y216F} (Y216F) cDNA into HCT-15 KO cells, and obtained the corresponding variants that expressed the WT or Y216F GSK3β proteins. As expected, reconstitution with WT-GSK3β, but not Y216F-GSK3β, partially restored the BRCA1 protein level (Figure 5D), suggesting that GSK3β enzymatic activity was required to retain protein. Ectopically expressed FLAG-GSK3β also resulted in an increase in BRCA1 protein in the parental HCT-15 cells, which further suggested a strong association between GSK3β and BRCA1 (Figure 5E).

The reduction in BRCA1 protein level appeared to be a result of transcriptional repression, as RT-PCR revealed that the *GSK3β* KO cells had reduced *BRCA1* mRNA expression (Figure 5F and Figure S4E). In addition, cells treated with GSK3i (CHIR99021 HCl and LY2090314) showed a reduced mRNA expression of *BRCA1* in a time- and concentration-dependent manner (Figure 5G and S4F). However, BRCA1 protein levels were not affected by MG132 treatment in *GSK3β* KO or GSK3i-treated cells (Figure 5H). Collectively, these data implied that GSK3β may repress BRCA1 transcription and protein expression in an enzyme-dependent manner.

PARPi and GSK3β inhibition are synergistic *in vivo*

Our data thus far indicated that GSK3 inhibition strongly synergizes with PARPi in BRCA2-deficient and BRCA1/2-proficient cancer cells *in vitro*. We further validated this therapeutic potential using xenograft mice models. BRCA2-deficient HCT-15 cells and BRCA-proficient RKO cells were subcutaneously injected into nude mice, and once tumor volume reached ~70 mm^3, either simmiparib or LY2090314, alone or in combination, was injected every other day for 14 d. Notably, the combination of these two agents significantly inhibited the growth of the tumor in the HCT-15 and RKO xenograft mouse model, although the tumor growth in the single agent groups was not affected following simmiparib or LY2090314 treatments (Figure 6A and 6B). Consistently, the tumor burden was significantly reduced as measured by the weight of dissected tumors (Figure 6C and 6D). The increased response to the combination treatment was associated with increased number of DSBs lesions (as indicated by γH2AX levels), as well as increased the levels of cleaved-Caspase3 in the combined treatment group (Figure 6E and 6F). In support of the mechanism identified in this study, the GSK3i group showed decreased BRCA1 protein level (Figure 6E and 6F). All the tested compounds caused no obvious loss of weight of the nude mice (Figure 6A and 6C) and were well tolerated during the drug administration.

To further validate the impact of GSK3β on *in vivo* sensitivity to PARPi, we used the HCT-15 *GSK3β* KO cells and parental cells to establish xenograft models in nude mice. As expected, administration of simmiparib significantly inhibited the growth of *GSK3β* KO tumor xenografts, but not the parental tumor xenografts. (Figure S5A and S5B). Consistently, there was a significant decrease in BRCA1 protein level and increase in γH2AX level in the *GSK3β* KO tumor xenografts treated with simmiparib (Figure S5C). These data demonstrated that inhibition or depletion of GSK3β could enhance the *in vivo* sensitivity to simmiparib without toxicity.

Discussion

To identify effective drug combinations for *BRCA*-mutated cancer cells with *de novo* PARPi resistance, we tested the cellular effect of a panel of compounds either alone or in combination with PARPi in *BRCA1*-mutated HCC1937 and *BRCA2*-mutated HCT-15 cells. Through this *in vitro* screen, we identified that a quarter of the oncological drugs and kinase inhibitors tested displayed synergy with PARPi in HCT-15 cells. These agents were included inhibitors of the DNA damage and cell cycle checkpoint (targeting ATR, CHK1 or CDK1), PI3K pathway (targeting PI3K, AKT or mTOR), and epigenetics regulators (targeting DNMT, HDAC and BET), and VEGFR. More importantly, the data suggested that GSK3 inhibition was most effective in enhancing the efficacy of PARPi. In conclusion, based on comprehensive and systematic screening of compounds, this study identified compounds that are capable of synergizing with PARPi.

Some of the synergistic interactions described in our screening were identified in previous studies [9, 10, 24–26, 28–30, 32]. For example, PARP inhibition was shown to synergize with: 1) PI3K pathway antagonism in BRCA-proficient triple-negative breast cancer cells, 2) ATR-Chk1 inhibition in PARPi-resistant BRCA-deficient cancer cells and high-grade serous ovarian cancer cells, 3) BET inhibition in

multiple tumor lineages, 4) VEGFR antagonism in ovarian cancer cells. Our screens also revealed that the synergistic effect between PARPi and these compounds was far more prevalent in BRCA2-deficient HCT-15 cells (~ 25%) than in BRCA1-deficient HCC1937 cells (~ 4%), which implicated that populations with *BRCA1* or *BRCA2* mutations may benefit differently from PARPi-based combination therapies.

GSK3, a serine/threonine protein kinase with two functionally distinct isoforms, α and β, was discovered in the context of glycogen metabolism and has emerged as a ubiquitous regulator of multiple signaling pathways [34, 35]. Historically, GSK3β has been thought of as a potential tumor suppressor due to its regulatory effect in the Wnt/β-catenin pathway [38]. However, large and ever increasing bodies of published data over the past decade have demonstrated that GSK3β is a positive regulator of cancer cell proliferation and survival in multiple tumor types [39]. CRC cells also displayed aberrant GSK3β expression and activity [40–42]. Direct pharmacologic inhibition of GSK3β signaling is, therefore, considered an attractive clinical strategy for these diseases [39]. A large number of GSK3i have entered clinical trials and several patent applications have been filed and/or granted [43]. Unfortunately, GSK3i have shown limited benefits, as monotherapy, in preclinical and clinical studies [44–48]. However, they appeared to be more effective when combined with other drugs [45, 49–52]. Here, our data showed strong synergistic effect between GSK3i and PARPi was observed in multiple CRC cell lines with diverse genetic backgrounds. Further *in vivo* studies showed that this new combination markedly suppressed tumor growth of HCT-15 and RKO tumor xenografts, without additional toxicity. Previous studies have demonstrated that olaparib combined with irinotecan displayed high toxicity concerns and no antitumor efficacy in CRC patients [53]. In this study, our results suggested that the combination of GSK3i and PARPi may produce encouraging responses with optimum tolerance in CRC patients.

In addition to regulating cellular processes including metabolism, growth, and survival, GSK3β also mediates the repair of DNA DSBs through phosphorylation of p53 binding protein 1 (53BP1) [54] and modulates the HRR pathway by phosphorylating the Fanconi anemia-associated protein (FAAP2), an important component of the Fanconi anemia complex involved in the repair of DNA interstrand cross-links [55]. Furthermore, GSK3i altered the level of proteins involved in DNA repair, such as, ATR-interacting protein (ATRIP), topoisomerase IIβ binding protein (TopBP1) [51], tumor protein p53-induced nuclear protein 1 (TP53INP1) [52], and Tap63 [56]. In addition, GSK3β inhibition has been shown to enhance ionizing radiation-based sensitivity in vitro [57] and in xenograft models [54]. Our results advanced the current understanding of role of GSK3β by showing that GSK3β is essential for DSBs in HRR by affecting BRCA1 mRNA and protein expression. This mechanism was observed in all the cell lines with variable responses to the combination of GSK3 and PARP inhibition. However, the protein expression of BRCA1 was almost completely abrogated, while the mRNA level of *BRCA1* only decreased to ~ 50% upon GSK3β inhibition and depletion, suggesting the involvement of other possible mechanisms. Therefore, the mechanism responsible for the suppression of BRCA1 expression by GSK3β remains to be further clarified.

Conclusion

Collectively, our data provide a mechanistic understanding of combined PARP and GSK3 inhibition in CRC cells. Pharmacological and genetic studies suggested that loss of GSK3β activity impaired HRR efficacy, suppressed BRCA1 mRNA and protein levels and substantially sensitized cells to PARPi and Top I inhibitors in replication-dependent DSBs lesions. Our study implies that GSK3β is an important modulator of HRR. Notably, GSK3i may be combined with PARPi-based treatments in a wider population of CRC patients.

Abbreviations

ADR: adriamycin

ATRIP: ATR-interacting protein

CHIR: CHIR99021 HCl

CI: combination index

CPT-11: irinotecan

CRC: colorectal cancer

DSBs: DNA double-strand breaks

FAAP2: fanconi anemia-associated protein

GSK3: glycogen synthase kinase 3

HRR: homologous recombination repair

HR: homologous recombination

IR: inhibition rate

LY: LY2090314

NP: niraparib

OP: olaparib

PARP: poly ADP-ribose polymerase

PARPi: PARP inhibitors

RP: rucaparib

SD: standard deviation

SP: simmiparib

STR: short tandem repeat

SRB: Sulforhodamine B

TopBP1: topoisomerase IIβ binding protein

TP: talazoparib

TP53INP1: tumor protein p53-induced nuclear protein 1

VP-16: etoposide

WT: wild type

53BP1: p53 binding protein 1

Declarations

Acknowledgements

None.

Funding

This work was supported by grants from the National Natural Science Foundation of China (81773764 to J.X. He), the Chinese Academy of Sciences (29201731121100101 to J.X. He and XDA12020104, XDA12020109 and CASIMM0120185003 to Z.H. Miao), the Science and Technology Commission of Shanghai Municipality (19QA1410900 to J.X. He), the State Key Laboratory of Drug Research and, and SA-SIBS Scholarship Program.

Authors' contributions

ZN performed most experiments, analyzed the data and wrote the manuscript; TYN participated in the cell viability assay; ZLN, LMZ and BXB participated in the animal experiments; SSS and HXJ supervised the work and provided administrative support; HXJ designed the overall study, supervised the experiments, analyzed the results, and wrote the paper. All authors read and approved the final manuscript.

Availability of data and materials

All data generated or analyzed during this study are included either in this article or in the supplementary information files.

Ethics approval and consent to participate

This study was carried out in strict accordance with the recommendations in the Guidelines for the Care and Use of Laboratory Animals of the National Institutes of Health. All animal studies were conducted in compliance with the Institutional Animal Care and Use Committee guidelines of the Shanghai Institute of Materia Medica (Shanghai, China).

Consent for publication

Not applicable

Competing interests

The authors declare that they have no competing interests.

References

1. Wang YQ, Wang PY, Wang YT, Yang GF, Zhang A, Miao ZH. An update on poly (ADP-ribose) polymerase-1 (PARP-1) inhibitors: opportunities and challenges in cancer therapy. J Med Chem. 2016; 59:9575-9598.
2. Min A, Im SA. PARP inhibitors as therapeutics: beyond modulation of PARylation. Cancers. 2020; 1:16.
3. J de Bono J, Mateo J, Fizazi K, Saad F, Shore N, Sandhu S, Chi KN, Sartor O, Agarwal N, Olmos D. Olaparib for metastatic castration-resistant prostate cancer. N Engl J Med. 2020; 382:2091-2102.
4. Li H, Liu ZY, Wu N, Chen YC, Cheng Q, Wang J. PARP inhibitor resistance: the underlying mechanisms and clinical implications. Mol Cancer. 2020; 1:16.
5. Jonsson P, Bandlamudi C, Cheng ML, Srinivasan P, Chavan SS, Friedman ND, Rosen EY, Richards AL, Bouvier N, Selcuklu SD. Tumor lineage shapes BRCA-mediated phenotypes. Nature. 2019; 571:576-579.
6. Pilie PG, Tang C, Mills GB, Yap TA. State-of-the-art strategies for targeting the DNA damage response in cancer. Nat Rev Clin Oncol. 2019; 16:81-104.
7. Lynparza (olaparib) approved by FDA as first-line maintenance treatment with Bevacizumab for HDR-positive advanced ovarian cancer. 2020. https://bitly/3cft3tu. Accessed 8 May 2020.
8. Chen HD, Chen CH, Wang YT, Guo N, Tian YN, Huan XJ, Song SS, He JX, Miao ZH. Increased PARP1-DNA binding due to autoPARylation inhibition of PARP1 on DNA rather than PARP1-DNA trapping is correlated with PARP1 inhibitor's cytotoxicity. Int J Cancer. 2019; 145:714-727.
9. Yazinski SA, Comaills V, Buisson R, Genois MM, Nguyen HD, Ho CK, Todorova Kwan T, Morris R, Lauffer S, Nussenzweig A. ATR inhibition disrupts rewired homologous recombination and fork protection pathways in PARP inhibitor-resistant BRCA-deficient cancer cells. Genes Dev. 2017; 31:318-332.
10. Parmar K, Kochupurakkal BS, Lazaro JB, Wang ZC, Palakurthi S, Kirschmeier PT, Yang C, Sambel LA, Farkkila A, Reznichenko E, et al. The CHK1 inhibitor Prexasertib exhibits monotherapy activity in high-

grade serous ovarian cancer models and sensitizes to PARP inhibition. Clin Cancer Res. 2019; 25:6127-6140.

11. Oza AM, Cibula D, Benzaquen AO, Poole C, Mathijssen RHJ, Sonke GS, Colombo N, Špaček J, Vuylsteke P, Hirte H. Olaparib combined with chemotherapy for recurrent platinum-sensitive ovarian cancer: a randomised phase 2 trial. The Lancet Oncology. 2015; 16:87-97.
12. Kummar S, Chen A, Ji J, Zhang Y, Reid JM, Ames M, Jia L, Weil M, Speranza G, Murgo AJ, et al. Phase I study of PARP inhibitor ABT-888 in combination with topotecan in adults with refractory solid tumors and lymphomas. Cancer Res. 2011; 71:5626-5634.
13. Middleton MR, Friedlander P, Hamid O, Daud A, Plummer R, Falotico N, Chyla B, Jiang F, McKeegan E, Mostafa NM. Randomized phase II study evaluating veliparib (ABT-888) with temozolomide in patients with metastatic melanoma. Ann Oncol. 2015; 26:2173-2179.
14. Bendell J, O'Reilly EM, Middleton MR, Chau I, Hochster H, Fielding A, Burke W, Burris H. Phase I study of olaparib plus gemcitabine in patients with advanced solid tumors and comparison with gemcitabine alone in patients with locally advanced/metastatic pancreatic cancer. Ann Oncol. 2015; 26:804-811.
15. Keung MY, Wu Y, Badar F, Vadgama JV. Response of breast cancer cells to PARP inhibitors is independent of BRCA status. J Clin Med. 2020; 1:15.
16. Atsushi Osoegawa JJG, Shigeru Kawabata and Phillip A. Rapamycin sensitizes cancer cells to growth inhibition by the PARP inhibitor olaparib. Oncotarget. 2017; 8:87044-87053.
17. Yuan B, Ye N, Song SS, Wang YT, Song Z, Chen HD, Chen CH, Huan XJ, Wang YQ, Miao ZH. Poly (ADP-ribose) polymerase (PARP) inhibition and anticancer activity of simmiparib, a new inhibitor undergoing clinical trials. Cancer Lett. 2017; 386:47-56.
18. Ye N, Chen CH, Chen T, Song Z, He JX, Huan XJ, Song SS, Liu Q, Chen Y, Ding J. Design, synthesis, and biological evaluation of a series of benzo[de][1,7]naphthyridin-7(8H)-ones bearing a functionalized longer chain appendage as novel PARP1 inhibitors. J Med Chem. 2013; 56:2885-2903.
19. Chen WH, Song SS, Qi MH, Huan XJ, Wang YQ, Jiang H, Ding J, Ren GB, Miao ZH, Li J. Discovery of potent 2,4-difluoro-linker poly (ADP-ribose) polymerase 1 inhibitors with enhanced water solubility and in vivo anticancer efficacy. Acta Pharmacol Sin. 2017; 38:1521-1532.
20. Chou TC. Drug combination studies and their synergy quantification using the Chou-Talalay method. Cancer Res. 2010; 70:440-446.
21. Yi JM, Huan XJ, Song SS, Zhou H, Wang YQ, Miao ZH. Triptolide induces cell killing in multidrug-resistant tumor cells via CDK7/RPB1 rather than XPB or p44. Mol Cancer Ther. 2016; 15:1495-1503.
22. Yang ZM, Liao XM, Chen Y, Shen YY, Yang XY, Su Y, Sun YM, Gao YL, Ding J, Zhang A, Miao ZH. Combining 53BP1 with BRCA1 as a biomarker to predict the sensitivity of poly (ADP-ribose) polymerase (PARP) inhibitors. Acta Pharmacol Sin. 2017; 38:1038-1047.
23. Andrew J. Pierce RDJ, Larry H. Thompson,and Maria Jasin. XRCC3 promotes homology-directed repair of DNA damage in mammalian cells. GENES & DEVELOPMENT. 1999; 13:2633-2638.

24. Lu Yang YZ, Weiwei Shan. Repression of BET activity sensitizes homologous recombination–proficient cancers to PARP inhibition. Sci Transl Med. 2017; 1:12.
25. Johnson N, Li Y-C, Walton ZE, Cheng KA, Li D, Rodig SJ, Moreau LA, Unitt C, Bronson RT, Thomas HD. Compromised CDK1 activity sensitizes BRCA-proficient cancers to PARP inhibition. Nature Medicine. 2011; 17:875-882.
26. Chao OS, Goodman OB, Jr. Synergistic loss of prostate cancer cell viability by coinhibition of HDAC and PARP. Mol Cancer Res. 2014; 12:1755-1766.
27. Jiang J, Lu Y, Li Z, Li L, Niu D, Xu W, Liu J, Fu L, Zhou Z, Gu Y, Xia F. Ganetespib overcomes resistance to PARP inhibitors in breast cancer by targeting core proteins in the DNA repair machinery. Invest New Drugs. 2017; 35:251-259.
28. Ibrahim YH, Garcia-Garcia C, Serra V, He L, Torres-Lockhart K, Prat A, Anton P, Cozar P, Guzman M, Grueso J. PI3K inhibition impairs BRCA1/2 expression and sensitizes BRCA-proficient triple-negative breast cancer to PARP inhibition. Cancer Discov. 2012; 2:1036-1047.
29. Alanna R. Kaplan1, Susan E. Gueble. Cediranib suppresses homology-directed DNA repair through down-regulation of BRCA1/2 and RAD51. Sci Transl Med. 2019; 1:12.
30. Muvarak NE, Chowdhury K, Xia L, Robert C, Choi EY, Cai Y, Bellani M, Zou Y, Singh ZN, Duong VH. Enhancing the cytotoxic effects of PARP inhibitors with DNA demethylating agents - a potential therapy for cancer. Cancer Cell. 2016; 30:637-650.
31. Fok JHL, Ramos-Montoya A, Vazquez-Chantada M, Wijnhoven PWG, Follia V, James N, Farrington PM, Karmokar A, Willis SE, Cairns J. AZD7648 is a potent and selective DNA-PK inhibitor that enhances radiation, chemotherapy and olaparib activity. Nat Commun. 2019; 1:15.
32. Mo W, Liu Q, Lin CC, Dai H, Peng Y, Liang Y, Peng G, Meric-Bernstam F, Mills GB, Li K, Lin SY. mTOR inhibitors suppress homologous recombination repair and synergize with PARP inhibitors via regulating SUV39H1 in BRCA-proficient triple-negative breast cancer. Clin Cancer Res. 2016; 22:1699-1712.
33. Kukita A, Sone K, Oda K, Hamamoto R, Kaneko S, Komatsu M, Wada M, Honjoh H, Kawata Y, Kojima M. Histone methyltransferase SMYD2 selective inhibitor LLY-507 in combination with poly ADP ribose polymerase inhibitor has therapeutic potential against high-grade serous ovarian carcinomas. Biochem Biophys Res Commun. 2019; 513:340-346.
34. Woodgett JR. Molecular cloning and expression of glycogen synthase kinase-3/Factor A. EMBO J. 1990; 9:2431-2438.
35. Kaidanovich-Beilin O, Woodgett JR. GSK-3: functional insights from cell biology and animal models. Front Mol Neurosci. 2011; 4:40.
36. Rong-Guang Shao C-XC, Hongliang Zhang, Kurt W.Kohn, Marc S.Wold and Yves Pommier. Replication-mediated DNA damage by camptothecin induces phosphorylation of RPA by DNA-dependent protein kinase and dissociates RPA:DNA-PK complexes. The EMBO Journal. 1999; 18:1397-1406.

37. He JX, Yang CH, Miao ZH. Poly(ADP-ribose) polymerase inhibitors as promising cancer therapeutics. Acta Pharmacol Sin. 2010; 31:1172-1180.
38. Tejeda-Munoz N, Robles-Flores M. Glycogen synthase kinase 3 in Wnt signaling pathway and cancer. IUBMB Life. 2015; 67:914-922.
39. Walz A, Ugolkov A, Chandra S, Kozikowski A, Carneiro BA, O'Halloran TV, Giles FJ, Billadeau DD, Mazar AP. Molecular pathways: revisiting glycogen synthase kinase-3β as a target for the treatment of cancer. Clin Cancer Res. 2017; 23:1891-1897.
40. Mai W, Kawakami K, Shakoori A, Kyo S, Miyashita K, Yokoi K, Jin M, Shimasaki T, Motoo Y, Minamoto T. Deregulated GSK3β sustains gastrointestinal cancer cells survival by modulating human telomerase reverse transcriptase and telomerase. Clin Cancer Res. 2009; 15:6810-6819.
41. Shakoori A, Ougolkov A, Yu ZW, Zhang B, Modarressi MH, Billadeau DD, Mai M, Takahashi Y, Minamoto T. Deregulated GSK3β activity in colorectal cancer: its association with tumor cell survival and proliferation. Biochem Biophys Res Commun. 2005; 334:1365-1373.
42. Shakoori A, Mai W, Miyashita K, Yasumoto K, Takahashi Y, Ooi A, Kawakami K, Minamoto T. Inhibition of GSK-3β activity attenuates proliferation of human colon cancer cells in rodents. Cancer Sci. 2007; 98:1388-1393.
43. Palomo V, Martinez A. Glycogen synthase kinase 3 (GSK-3) inhibitors: a patent update (2014-2015). Expert Opin Ther Pat. 2017; 27:657-666.
44. Rizzieri DA, Cooley S, Odenike O, Moonan L, Chow KH, Jackson K, Wang X, Brail L, Borthakur G. An open-label phase 2 study of glycogen synthase kinase-3 inhibitor LY2090314 in patients with acute leukemia. Leuk Lymphoma. 2016; 57:1800-1806.
45. Gray JE, Infante JR, Brail LH, Simon GR, Cooksey JF, Jones SF, Farrington DL, Yeo A, Jackson KA, Chow KH. A first-in-human phase I dose-escalation, pharmacokinetic, and pharmacodynamic evaluation of intravenous LY2090314, a glycogen synthase kinase 3 inhibitor, administered in combination with pemetrexed and carboplatin. Invest New Drugs. 2015; 33:1187-1196.
46. Ugolkov A, Dubrovskyi O, Gaisina I, Yemelyanov A, Mazar A. Abstract 2699: targeting GSK-3: a novel approach to enhance glioblastoma chemosensitivity. Cancer Research. 2015; 75:2699-2699.
47. Wick W, Puduvalli VK, Chamberlain MC, van den Bent MJ, Carpentier AF, Cher LM, Mason W, Weller M, Hong S, Musib L. Phase III study of enzastaurin compared with lomustine in the treatment of recurrent intracranial glioblastoma. J Clin Oncol. 2010; 28:1168-1174.
48. Kreisl TN, Kotliarova S, Butman JA, Albert PS, Kim L, Musib L, Thornton D, Fine HA. A phase I/II trial of enzastaurin in patients with recurrent high-grade gliomas. Neuro Oncol. 2010; 12:181-189.
49. Ugolkov A, Gaisina I, Zhang JS, Billadeau DD, White K, Kozikowski A, Jain S, Cristofanilli M, Giles F, O'Halloran T. GSK-3 inhibition overcomes chemoresistance in human breast cancer. Cancer Lett. 2016; 380:384-392.
50. Curtis A Thorne CW, Adam D Coster, Bruce A Posner, Lani F Wu & Steven J Altschuler. GSK-3 modulates cellular responses to a broad spectrum of kinase inhibitors. Nature Chemical Biology. 2015; 11:58-63.

51. Ding L, Madamsetty VS, Kiers S, Alekhina O, Ugolkov A, Dube J, Zhang Y, Zhang JS, Wang E, Dutta SK. Glycogen synthase kinase-3 inhibition sensitizes pancreatic cancer cells to chemotherapy by abrogating the TopBP1/ATR-mediated DNA damage response. Clin Cancer Res. 2019; 25:6452-6462.
52. Shimasaki T, Ishigaki Y, Nakamura Y, Takata T, Nakaya N, Nakajima H, Sato I, Zhao X, Kitano A, Kawakami K. Glycogen synthase kinase 3β inhibition sensitizes pancreatic cancer cells to gemcitabine. J Gastroenterol. 2012; 47:321-333.
53. Chen EX, Jonker DJ, Siu LL, McKeever K, Keller D, Wells J, Hagerman L, Seymour L. A Phase I study of olaparib and irinotecan in patients with colorectal cancer: canadian cancer trials group IND 187. Invest New Drugs. 2016; 34:450-457.
54. Yang Y, Lei T, Du S, Tong R, Wang H, Yang J, Huang J, Sun M, Wang Y, Dong Z. Nuclear GSK3β induces DNA double-strand break repair by phosphorylating 53BP1 in glioblastoma. Int J Oncol. 2018; 52:709-720.
55. Jingming Wang UJ, So Young Joo and Hyungjin Kim. FBW7 regulates DNA interstrand cross-link repair by modulating FAAP20 degradation. Oncotarget. 2016; 7:24.
56. Wen J, Yan H, He M, Zhang T, Mu X, Wang H, Zhang H, Xia G, Wang C. GSK-3β protects fetal oocytes from premature death via modulating TAp63 expression in mice. BMC Biol. 2019; 17:23.
57. Kitano A, Shimasaki T, Chikano Y, Nakada M, Hirose M, Higashi T, Ishigaki Y, Endo Y, Takino T, Sato H. Aberrant glycogen synthase kinase 3β is involved in pancreatic cancer cell invasion and resistance to therapy. PLoS One. 2013; 1:13.

Figures

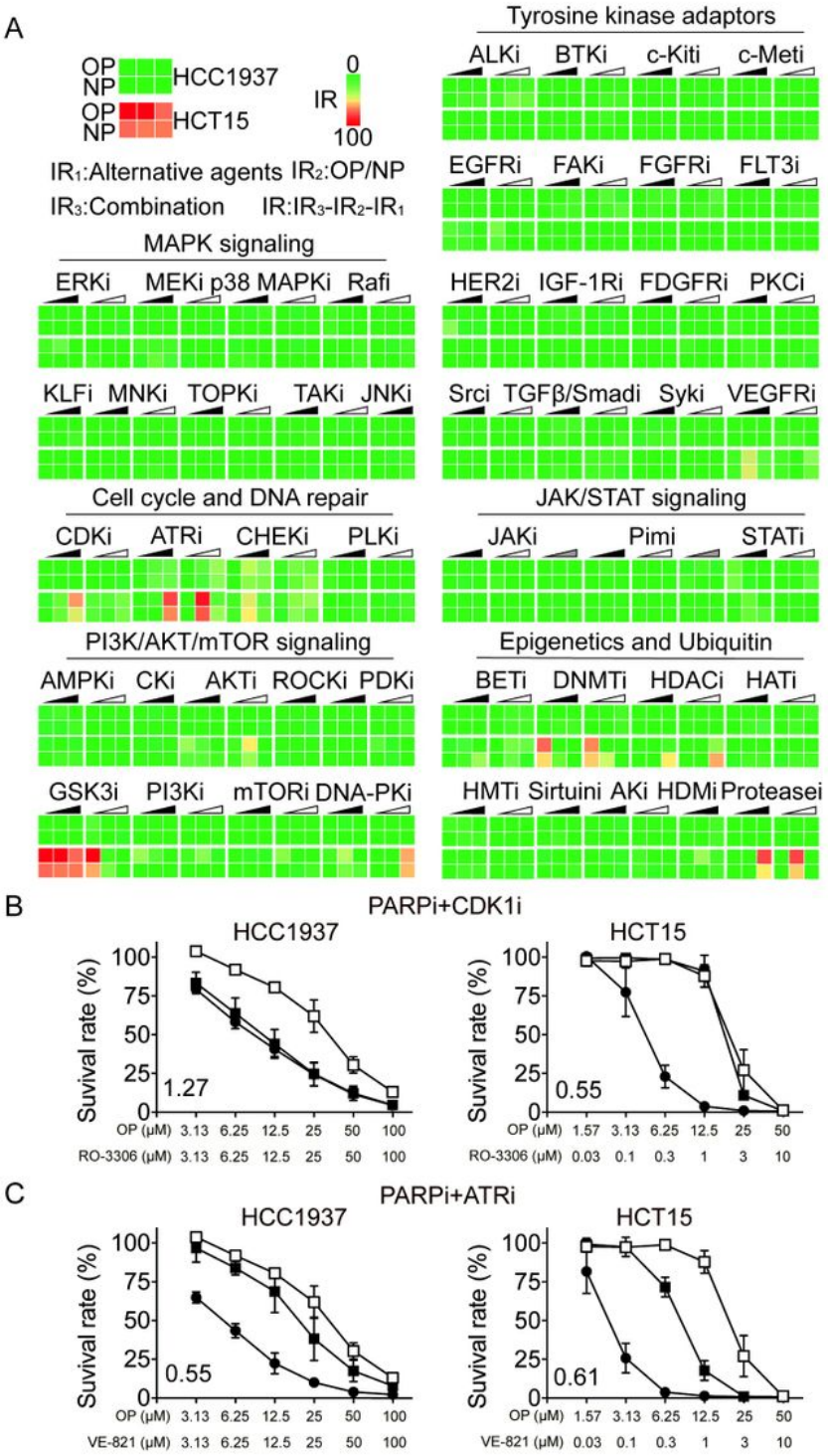

Figure 1

Drug combination screen identifies GSK3i as acting synergistically with PARPi A, Heatmap representation of the efficacy of drugs combinations. Screening of drug combinations was performed in BRCA1-deficient HCC1937 and BRCA2-deficient HCT-15 cells. Cells were treated with 99 agents at three concentrations covering a 100-fold concentration range, with or without the PARP inhibitors (PARPi, olaparib [OP] or niraparib [NP]) at a concentration of about 20% inhibition rate (IR). The IRs of the indicated agent, PARPi

and combination were defined as IR1, IR2 and IR3, respectively. The color-coding denotes the level of IR (green [0% inhibition] to red [100% inhibition]) which was calculated as IR3-IR2-IR1. B and C, Effect of single agent and combination treatment on HCT-15 cell viability for combinations of PARP inhibitor, olaparib, plus CDK1 inhibitor RO-3306 (B) or ATR inhibitor VE-821 (C). OP, olaparib. Cell viability was measured by Sulforhodamine B assay (SRB). Combination index (CI) was calculated using CalcuSyn software with the Chou-Talalay equation, and average CI value are presented (CI < 1, synergism; CI = 1, additive effect; CI > 1 antagonism). Data are from three independent experiments and expressed as mean ± standard deviation (SD).

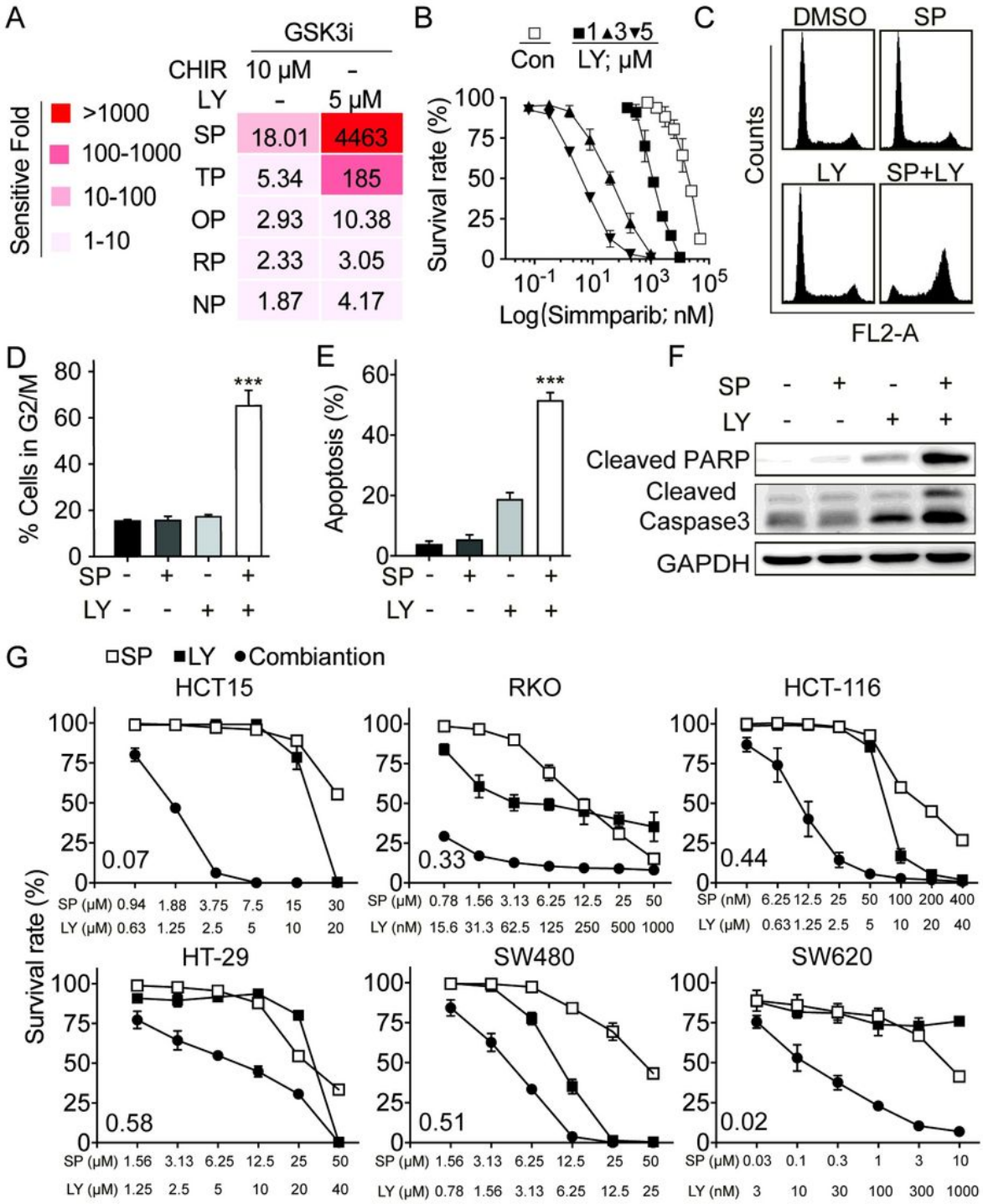

Figure 2

GSK3 inhibition sensitizes BRCA-proficient CRC cells to PARPi A, Change in sensitivity to PARPi when combined with GSK3i. HCT-15 cells were treated with various PARPi, including simmiparib, talazoparib, rucaparib, olaparib, and niraparib, without or with specific GSK3i CHIR99021 HCl (10 μM) or LY2090314 (5 μM) for 7 d. SP, simmiparib; TP, talazoparib; OP, olaparib; RP, rucaparib; NP, niraparib; CHIR, CHIR99021 HCl; and LY, LY2090314. Data (fold-sensitivity) are presented as the ratio of (IC50 of PARPi)/(IC50 of

PARPi plus GSK3i), indicating a reduction in IC50 of PARPi in the presence of GSK3i. Color intensity represents the value of the fold-sensitivity. B, Dose-response curves for HCT-15 cells treated with the indicated concentration of simmiparib with or without the LY2090314 (LY: 1, 3 and 5 μM) for 7 d. C and D, G2/M arrest induced by single-agents or the indicated combination in HCT-15 cells was determined using FACS. Cells were treated with 5 μM simmiparib, 5 μM LY2090314 or a combination for 48 h and then subjected to FACS analysis. C, Representative histograms are shown. D, Percentage of cells in the G2/M phase expressed as mean ± SD from three independent experiments are shown. ***, $p < 0.001$. E, Apoptosis induced by single-agents or the indicated combination in HCT-15 cells. Cells were treated with 5 μM simmiparib, 5 μM LY2090314 or a combination for 72 h and then analyzed using annexin V-FITC-PI-staining-based flow cytometry. ***, $p < 0.001$. F, Expression of apoptosis-related proteins in HCT-15 cells exposed to single agent or the indicated combination detected by western blotting. G, GSK3 inhibitor, LY2090314, sensitized cells to PARP inhibitor, simmiparib, in a panel of cells. The survival fraction and the average of CI are shown from three independent experiments. SP, simmiparib; LY, LY2090314.

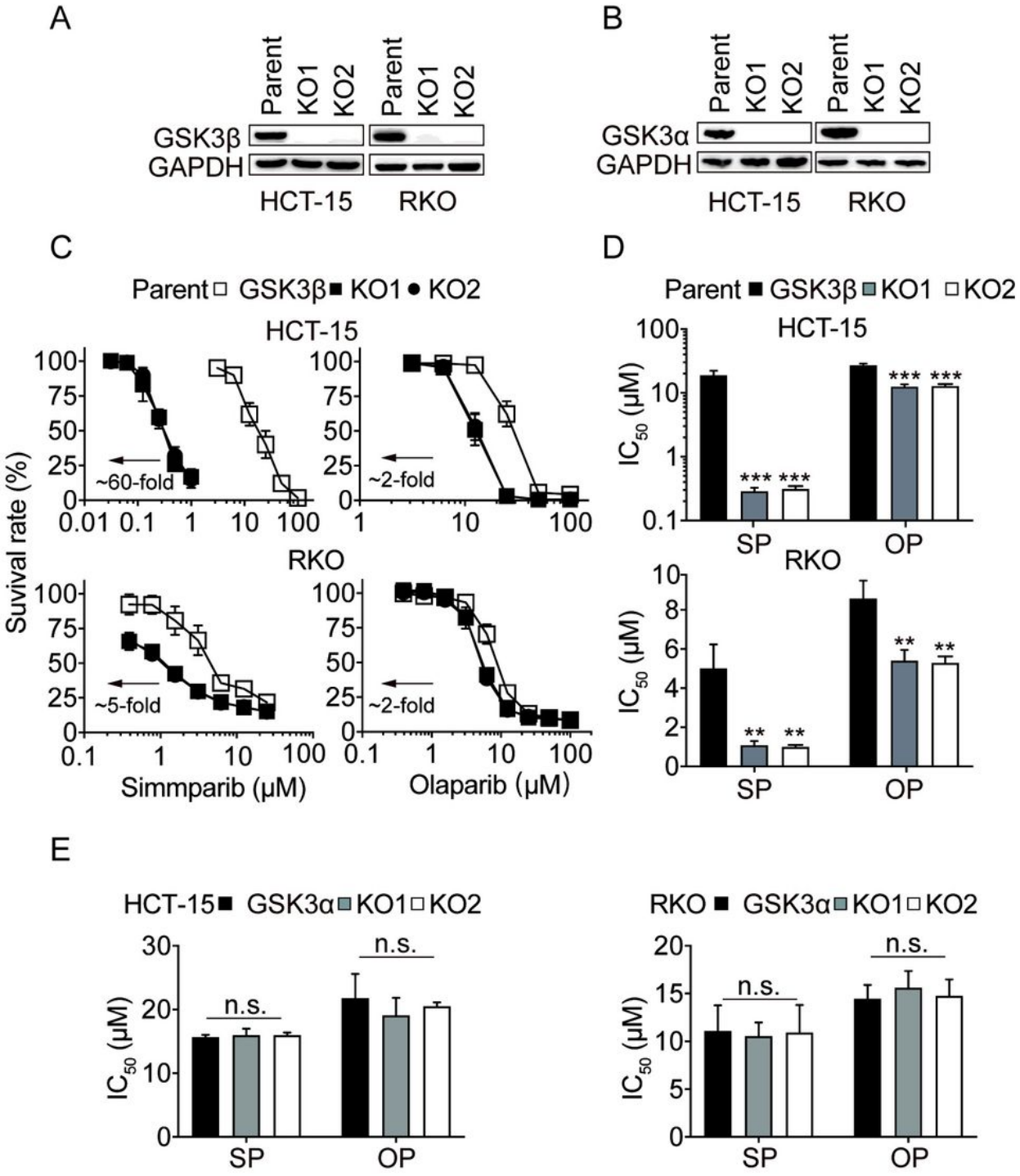

Figure 3

GSK3β depletion selectively sensitizes cancer cells to PARP and Top I inhibitors A and B, Levels of GSK3β and GSK3α protein in different GSK3β-/- or GSK3α-/- clonal variants (KO1 and KO2) of HCT-15 and RKO cells were detected using western blotting. C-E, Change in sensitivity to PARPi following GSK3β (C and D) or GSK3α depletion (E). Cells were treated with simmiparib (SP) and olaparib (OP) for 7 d then subjected

to SRB assays. The IC50 values are expressed as mean ± SD from three independent experiments. **, p < 0.01; ***, p < 0.001; n.s. not significant.

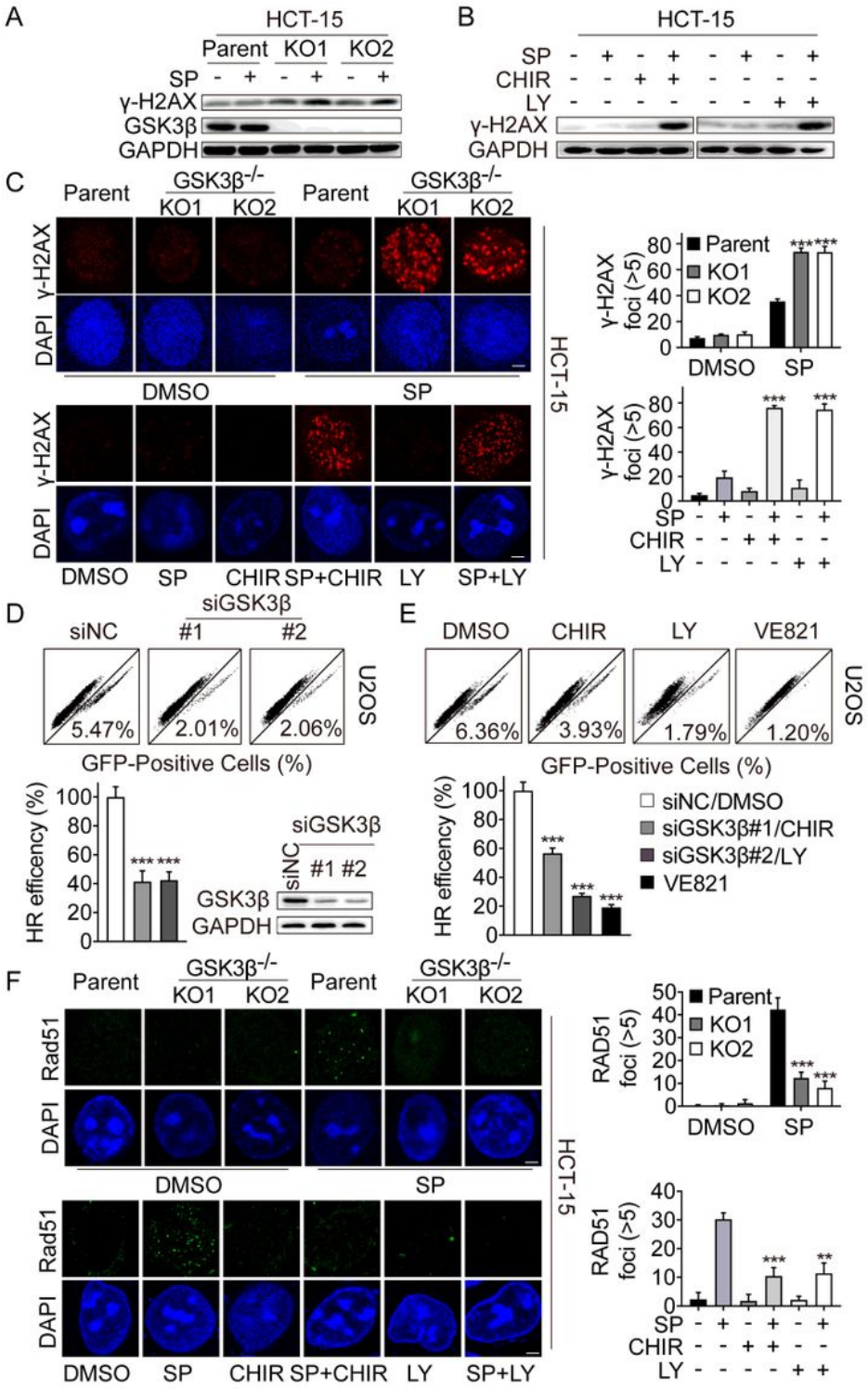

Figure 4

GSK3β is required for the homologous recombination repair of DSBs A, Western blot analysis of γH2AX in HCT-15 cells (parent) or corresponding GSK3β-depleted single clone (KO1 and KO2) cells treated with 5 μM simmiparib for 48 h. B, Western blot analysis of γH2AX in HCT-15 cells treated with 5 μM simmiparib,

GSK3i (10 μM CHIR99021 HCl or 5 μM LY2090314), or a combination for 48 h. C, Representative images of γH2AX foci in GSK3β KO cells (KO1 and KO2; Upper) or HCT-15 (parent cells; Lower) cells following treatment with 5 μM simmiparib, GSK3i (10 μM CHIR99021 HCl or 5 μM LY2090314), or a combination for 48 h. Nuclei were stained with DAPI. Scale bar: 2 μm. Cells that contained five or more γH2AX foci/nucleus were considered as γH2AX-positive cells. D and E, DR-U2OS cells were treated with siRNA, GSK3β inhibition (5 μM CHIR99021 HCl or 5 μM LY2090314) or positive control of VE821 (5 μM) for 24 h, followed by I-SceI transfection. GFP-positive cells were analyzed by flow cytometry 48 h later. F, Representative images of RAD51 foci in GSK3β KO (KO1 and KO2; Upper) or HCT-15 (parent cells; Lower) cells following treatment with 5 μM simmiparib, GSK3i (10 μM CHIR99021 HCl or 5 μM LY2090314), or a combination for 48 h. Scale bar: 2 μm. Cells that contained five or more RAD51 foci/nucleus were considered as RAD51-positive cells. All data are expressed as mean ± SD from three independent experiments. SP, simmiparib; CHIR, CHIR99021 HCl; LY, LY2090314. **, $p < 0.01$; ***, $p < 0.001$.

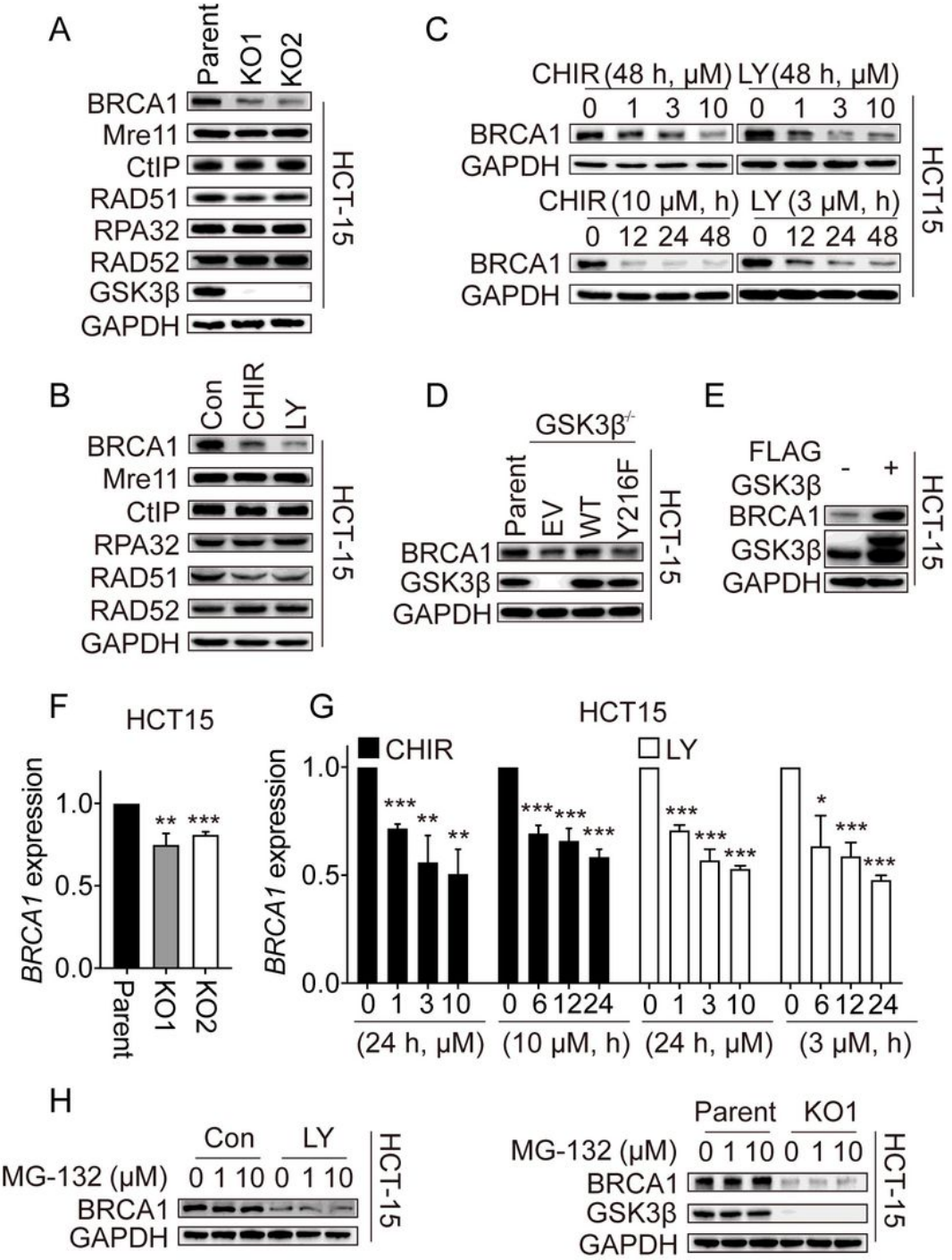

Figure 5

GSK3β depletion represses the expression of BRCA1 A, Levels of DNA repair-related proteins in the parental HCT-15 and their GSK3β KO cells determined by western blotting. B, Levels of DNA repair-related proteins in HCT-15 cells following treatment with 10 μM CHIR99021 HCl or 5 μM LY2090314 determined for 48 h by western blotting. CHIR, CHIR99021 HCl; and LY, LY2090314. C, BRCA1 protein levels in HCT-15 cells treated with GSK3i, CHIR99021 HCl and LY2090314, for indicated times and concentrations. CHIR,

CHIR99021 HCl; and LY, LY2090314. D, BRCA1 protein level was partially restored in HCT-15 GSK3β-depleted cells transfected with full-length WT-GSK3β cDNA (WT) but not with mutated-GSK3β cDNA (Y216F). E, Exogenous expression of GSK3β in HCT-15 cells increased BRCA1 protein level. F and G, mRNA expression of BRCA1 in the parental HCT-15 and GSK3β KO cells after treatment with the indicated drugs was detected by qRT-PCR. CHIR, CHIR99021 HCl; and LY, LY2090314. *, $p < 0.05$; **, $p < 0.01$; ***, $p < 0.001$. H, Treatment with MG132 failed to reverse the degradation of BRCA1 in HCT-15 and GSK3β KO cells. The indicated cells were treated with either LY2090314 or MG132 alone or in a combination for 24 h, and then the BRCA1 protein level was analyzed by western blotting. LY, LY2090314.

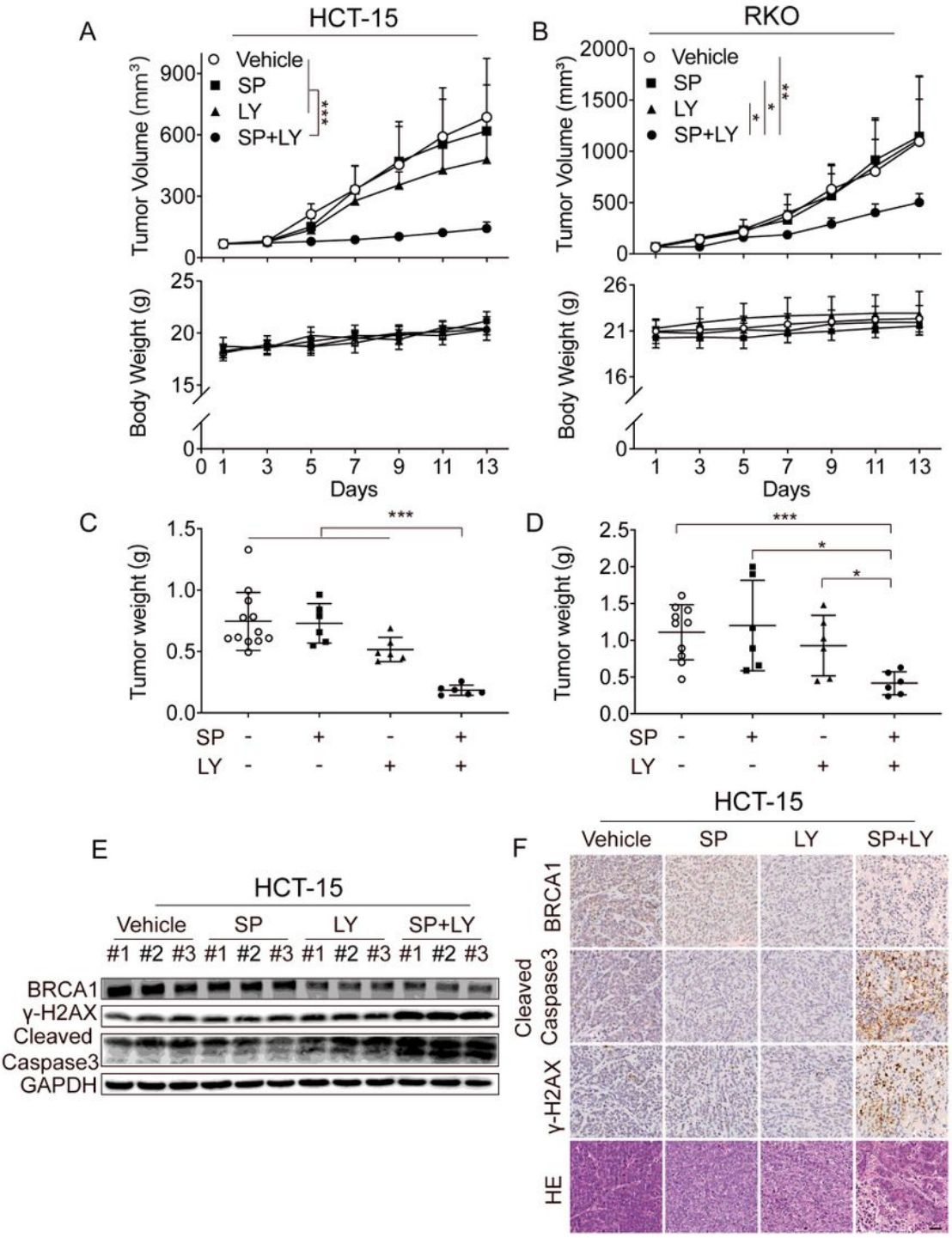

Figure 6

PARP and GSK3β inhibition are synergistic in vivo A-D, Mice bearing subcutaneous xenografts were treated with simmiparib (i.v.) or LY2090314 (i.v.) every other day, either alone or in a combination. Tumor volume, body weight and tumor weight were separately plotted. A and C show the effect of simmiparib (50 mg/kg) and LY2090314 (50 mg/kg), alone or in a combination on BRCA2-deficient HCT-15 xenografts; B and D show the effect of simmiparib (30mg/kg) and LY2090314 (30mg/kg), alone or in a

combination on BRCA-proficient RKO xenografts. E and F, Levels of BRCA1, γH2AX and cleaved-Caspase3 in HCT-15 xenografts determined by western blotting (E) or immunohistochemistry (F) analysis. Scale bar, 20 μm. SP, simmiparib; LY, LY2090314. *, $p < 0.05$; **, $p < 0.01$; ***, $p < 0.001$.

Supplementary Files

This is a list of supplementary files associated with this preprint. Click to download.

- TableS1Compoundsusedinthecombinationscreening.xls